scientific reports

Check for updates

OPEN

Study on the durability of solidified mud under chloride and dry-wet coupling

Zhang Songtao[1,2], Pang Jianyong[1]✉, Zhang Jinsong[1], Zhou Changwei[1] & Wang Yaxing[1]

In order to study the durability of solidified waste mud, dry-wet cycle experiments were carried out under the erosion of sodium chloride solutions with different concentrations. The unconfined compressive strength and mass change rate of solidified mud were studied and analyzed. The results show that when the number of dry-wet cycles increases, the unconfined compressive strength and mass of the sample show a downward trend. The unconfined compressive strength of the solidified mud in 40 g / L sodium chloride solution decreases the most, reaching 52.89%, and the mass loss reaches 8.36 g. The microstructure analysis was carried out by scanning electron microscopy. It was found that the hydration products such as hydrated calcium silicate gel (C-S-H) and calcium hydroxide crystal (C-H) in the solidified mud samples under the coupling of chloride erosion and dry-wet cycle were reduced, and more pores and cracks appeared. Under the same number of dry-wet cycles, the higher the concentration of sodium chloride solution, the more serious the micro-damage inside the sample. The decrease of the strength of the solidified slurry is due to the hydrolysis of the hydration products in the solidified mud under the combined action of chloride salt and dry-wet cycle, and some of the materials are dissolved, resulting in more cracks.

Keywords Chloride salt, Dry-wet cycle, Solidified mud, Unconfined compressive strength, Microstructure

During engineering construction, a significant amount of waste slurry is often generated. The indiscriminate discharge of this waste not only leads to resource wastage but also causes environmental pollution. Chemical curing methods for handling waste engineering slurry have become one of the most direct and effective common methods. Slurry treated by different curing methods can be utilized as filling material for drilled piles or road embankment materials, based on its mechanical and durability properties, thus transforming it into a construction material and achieving resource utilization[1–3].

Researchers both domestically and internationally have conducted a series of studies on slurry curing methods and achieved various applications in engineering. For instance, Wu et al.[4] proposed the "Silt-Bottom Slag Waste Material Matrix (MC-IBA Matrix)" for the "new soil" technology in land reclamation. Guan et al.[5] utilized different binding materials to cure soil, achieving the required curing performance and ensuring that the leachate concentrations of three heavy metals met hazardous waste landfill entry standards. Zentar et al.[6] investigated the curing effects of aluminosilicate fly ash and cement on seabed sediments. Yi et al.[7] studied the curing effect of alkaline-activated mineral powders on Lianyungang soft soil through laboratory mix ratio tests.

Ou et al.[8] applied microbial strains and their cultivation solutions to soil curing and investigated the curing effects, exploring the improvement mechanisms of microbes on the cured fill soil by analyzing the mineral composition and specific surface area of the cured soil. Additionally, researchers have studied the basic physical properties of cured slurry. Zhu et al.[9] studied the soil-water transfer mechanism during the cement curing of dredged sludge and explored the strength changes of the cured soil with cement addition. Huang et al.[10] investigated the stress-strain characteristics, compressive deformation, and strength characteristics of remolded and undisturbed cured sludge and compared the characteristics of the two[11]. Chan et al.[12] conducted a comprehensive parameter analysis of the physical and chemical properties of fill soil from Malaysian waters after curing with fly ash and cement. Chen[13] carried out a correlation study on the calcination temperature of sand washing slurry (SWS) and the ratio of alkaline solution on the microstructure and mechanical properties of SWS base polymers, which showed that a certain ratio of alkaline solution promoted the formation of more amorphous materials and enhanced the strength of the geopolymer compounds.

Many scholars have conducted a series of studies on slurry curing technology, aiding in the reapplication of engineering waste slurry in practical projects. In actual applications, due to the variability of natural environments,

[1]School of Civil Engineering and Architecture, Anhui University of Science and Technology, AnHui Huainan 232001, China. [2]Anhui Water Resources Development Co., Ltd, AnHui Bengbu 233000, China. ✉email: jypang@aust.edu.cn

engineering waste slurry often encounters dry-wet cycles due to rainfall and fluctuations in surface water. Prolonged dry-wet cycling can damage the soil structure of cured slurry, reducing the cohesion between internal particles, leading to internal cracking and increased porosity. This, in turn, decreases the strength and durability of the cured slurry, preventing it from achieving its intended performance[14]. In Northwestern or coastal areas, the effects of dry-wet cycles are further compounded by salt-induced erosion[15,16].

Research on the effects of chloride salt dry-wet cycles on cured slurry has been conducted. He et al.[17] carried out experiments on the properties of cured sludge under saline erosion environments, including appearance and unconfined compressive strength, and explored the mechanisms of erosion solutions on cured sludge. Tu et al.[18] added fly ash, mineral powder, or silica powder to grouting materials and conducted erosion tests in seawater, finding that the service life of the materials was significantly extended. Di et al.[19,20] investigated the changes in strength of bentonite by varying the concentration of salt solutions, discovering that the internal friction angle of residual strength increased with higher salt solution concentrations. Bian et al.[21] used laboratory simulation methods to study the durability evolution of polymer superabsorbent resin-cured silt under alternating dry-wet conditions and explored the effects of different SAP dosages, liquid limits, and kaolinite content on its basic physical properties (dry density, mass loss rate) and strength. While many scholars have made significant contributions to the study of salt-induced erosion and dry-wet cycling on cured slurry characteristics, there is limited research on the durability of cured slurry under the combined effects of chloride salt erosion and dry-wet cycles, and the results are not yet comprehensive. Therefore, it is necessary to continue studying the durability of cured slurry under the combined effects of chloride salt erosion and dry-wet cycles.

This paper conducts experimental research on the durability of cured slurry under the synergistic effects of chloride salt solutions of different concentrations and dry-wet cycles, and analyzes the microscopic structural changes under these conditions using scanning electron microscopy. The aim is to reveal the durability mechanisms of cured slurry and provide theoretical references for practical engineering applications.

Experimental materials and methods

Experimental materials

The bentonite used in this experimental slurry preparation is sodium bentonite, sourced from Sichuan Renshou County, with the composition detailed in Table 1. The soda produced in Tianjin Binhai New Area, with the main component being sodium carbonate (Na_2CO_3); the experimental sand is Xiamen, China ISO standard sand produced by Aisio Standard Sand Co., Ltd, with particle sizes ranging from 0.08 to 2 mm; the thickening agent selected is sodium carboxymethylcellulose (CMC), model FVH9 high viscosity. The primary curing material, slag, is s105 slag powder produced by Lingshou County Dehang Mineral Products Co., Ltd, mainly composed of $Ca_2Al_2SiO_7$ and Ca_2MgSiO_7 crystals; lime is purchased from Xinyu, Jiangxi Province, primarily composed of CaO with a content of 90.5%, and it is a high-calcium quicklime, produced from raw materials with calcium carbonate as the main ingredient and CO_2 is discharged through proper calcination. The chemical composition of slag and lime is presented in Table 1. The exciter water glass is industrial liquid sodium silicate, conforming to the quality standard of GB/T4209-2008 industrial sodium silicate, with a modulus of 2.3. The water used for the experiment is pure water without chlorine ions; the sodium chloride is analytically pure, with a content of not less than 99.5%, produced by Tianjin Kemi Chemical Reagent Co[22]. The relevant characteristics of the experimental materials are shown in Fig. 1.

Preparation of slurries for the experiments22

The engineering slurry used in this experiment is prepared manually in the laboratory, combined with the actual engineering slurry ratio and domestic scholars' research on bentonite slurry preparation[23]. The slurry composition, by mass ratio, is set as water: bentonite: soda ash: CMC = 100: 12: 0.5: 0.06. The slurry preparation should be fully stirred, rubbing undissolved or piled-up bentonite clay at the bottom until it is fully dissolved and sediment-free at the bottom, then stored in a cool place indoors for standby use. The materials are mixed over a period of three days. The formulated experimental slurry meets the indexes for engineering slurry use[24].

Preparation and maintenance of cured mud specimens

A 50 mm × 50 mm × 50 mm cube test mold is used to create solidified mud samples. Materials are weighed according to the ratios established from previous test results. The total dosage of the curing agent is 25%, with a mass ratio of slag to lime set at 17:3. Additionally, the dosages of water glass and sand are 5% and 40% of the mud mass, respectively. Solidified materials are accurately weighed and mixed in a mixing pot using a spatula. Then, the previously prepared mud and water glass are weighed and poured into the mixing pot. A cement mortar mixer is used to stir the mixture for 5 min until it is uniformly blended. After mixing, the mixture is poured into the mold and tapped on a vibrating table. Once the sample preparation is complete, it is sealed with plastic wrap and placed in a standard curing room for 3 days before demolding. After demolding, the sample is labeled

Name	SiO_2	Al_2O_3	CaO	MgO	Na_2O	K_2O	FeO	Fe_2O_3	SO_3	loss
bentonite	71.2	18.52	0.82	0.54	1.56	0.98	0.32	0.12	—	5.94
slag	35.32	20.46	28.41	5.97	0.22	—	—	1.54	1.46	6.62
lime	2.25	0.93	90.5	1.78	0.6	—	—	0.85	0.9	2.19

Table 1. Chemical composition of the experimental materials %.

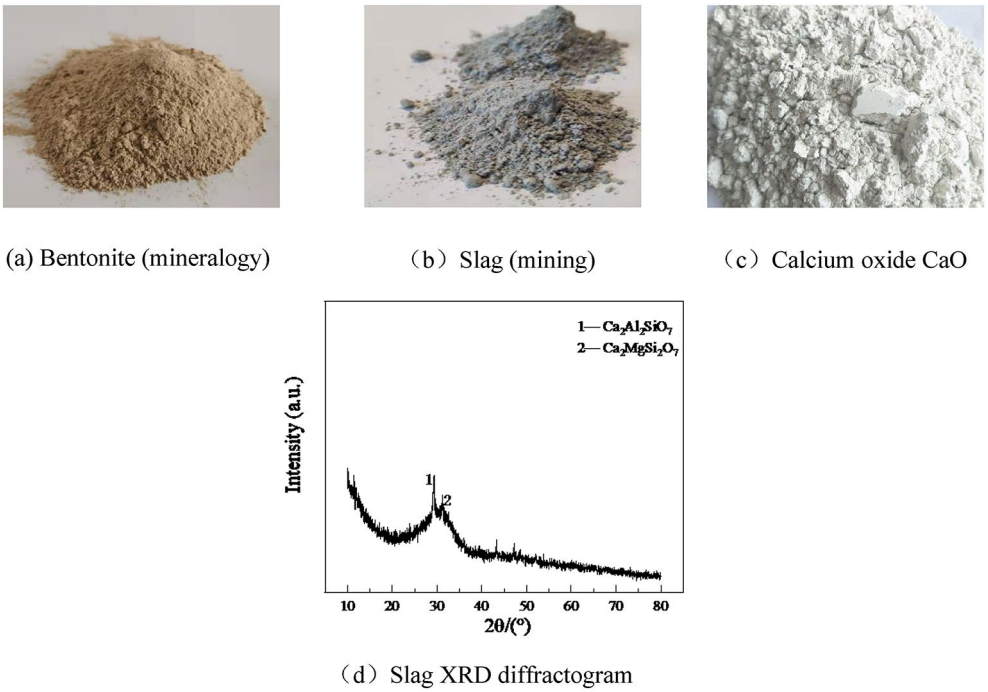

(a) Bentonite (mineralogy)　（b）Slag (mining)　（c）Calcium oxide CaO

（d）Slag XRD diffractogram

Fig. 1. Experimental materials

Fig. 2. Test sample

with a number, placed in a sealed bag, and then stored in a standard curing room for 28 days to prepare the test sample, as illustrated in Fig. 2.

Experimental methods

The chlorine salt corrosion and dry-wet cycle coupling test was conducted following the method outlined in ASTM D4843-88. The experimental samples were cured for 28 days. Once the curing age was reached, the samples were removed, numbered, and their initial mass was recorded after verifying that their appearance was intact. To initiate the test, each sample was first soaked in clean water and in three different concentrations of sodium chloride solutions: 10 g/L, 20 g/L, and 40 g/L for a duration of 12 h, with the water temperature maintained at 20 °C. A partially soaked sample is illustrated in Fig. 3. After soaking, the samples were removed, and any residual moisture on the surface was wiped off. Subsequently, the samples were placed in an electric constant-temperature drying oven set at 40 °C for 12 h, as shown in Fig. 4. This process completed one dry-wet cycle test. The designed number of dry and wet cycles included 1, 3, 5, 7, 9, 11, 13, and 15 cycles, along with a control group that was neither soaked nor subjected to dry and wet cycles, resulting in a total of 33 groups ($4\times8+1$). For each test set, three parallel specimens were prepared, culminating in a total of 99 specimens (3×3). Upon completion of the tests, the samples that had undergone the specified number of cycles were retrieved for physical assessments, including acoustic wave speed, apparent morphology, and mass. Following these assessments, an unconfined compressive strength test was conducted on each sample in accordance with the "Standard for Geotechnical Test Methods" (GB/T50123-1999). The WAW-1000 microcomputer-controlled electro-hydraulic servo universal testing machine was utilized for this test, employing the constant velocity displacement loading method with a preload set to 0.05 KN and a loading rate of 1 mm/min. After the test, a scanning electron microscope test was used to analyze the microscopic mechanism of some samples. The test flow chart is shown in Fig. 5.

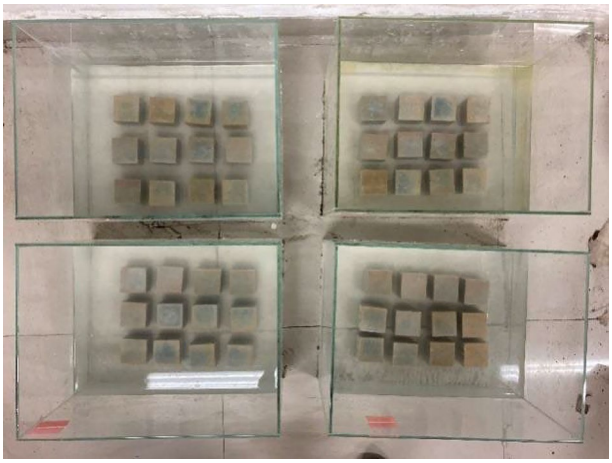

Fig. 3. Partially soaked specimen.

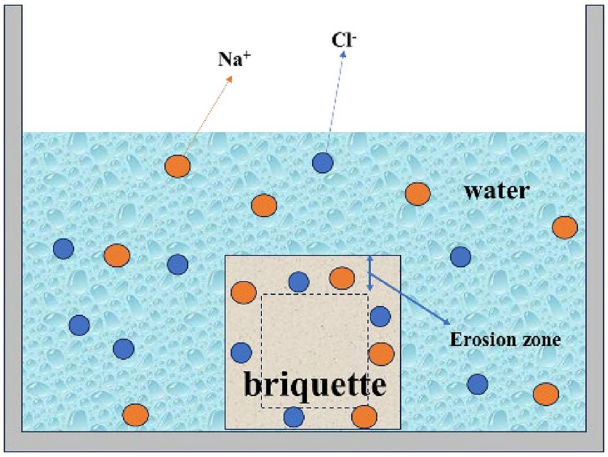

Fig. 4. Schematic diagram of the immersion environment.

Test results and analysis

Non-destructive testing of internal defects

The longitudinal wave velocity is an important indicator to measure the internal density of a material. Its function is to reflect the changes in the pore structure and the development of cracks inside the material by measuring changes in wave velocity[25–27]. Therefore, by measuring the longitudinal wave velocity of the solidified mud, it can reflect the degree of damage inside the sample. Figure 6 shows the relationship between the longitudinal wave velocity of solidified mud and the number of dry-wet cycles under the action of chlorine salt and dry-wet coupling.

As can be seen in Fig. 6, the longitudinal wave velocity of the cured mud specimens immersed in water and different concentrations of sodium chloride solution showed a general trend of rapid decrease and then slow decrease and leveling off with the increase in the number of wet and dry cycles. After two wet and dry cycles, compared with the control group without testing, the decrease of the longitudinal wave velocity of the samples was the largest, in which the longitudinal wave velocity of the samples in water and 10 g/L, 20 g/L, 40 g/L NaCl solution decreased by 56.12%, 49.47%, 47.52%, and 45.22%, respectively; the decreasing trend of longitudinal wave velocity of the samples slowed down in the 2–6 wet and dry cycles, and the decrease of longitudinal wave velocity in the 2–6 wet and dry cycles slowed down, and the decreasing trend of longitudinal wave velocity in the 2–3 wet and dry cycles slowed down. Compared with 2 times of wet and dry cycles, the longitudinal wave velocity of the specimen after 4 times of wet and dry cycles decreased by 20.06%, 20.34%, 21.71%, and 12.36% in water and 10 g/L, 20 g/L, 40 g/L NaCl solution, respectively; the change of longitudinal wave velocity of the specimen tended to be flat in 6 ~ 10 times of wet and dry cycles and partly fluctuating, which indicated that the longitudinal wave velocity of the specimen gradually tended to be stable at this time. This indicates that the longitudinal wave speed of the specimen gradually tends to stabilize. The reason for this phenomenon is that after the wet and dry cycles of the specimen due to the action of freezing and thawing expansion and contraction of the specimen caused by the gradual increase in the pores and cracks inside the specimen, and due to the

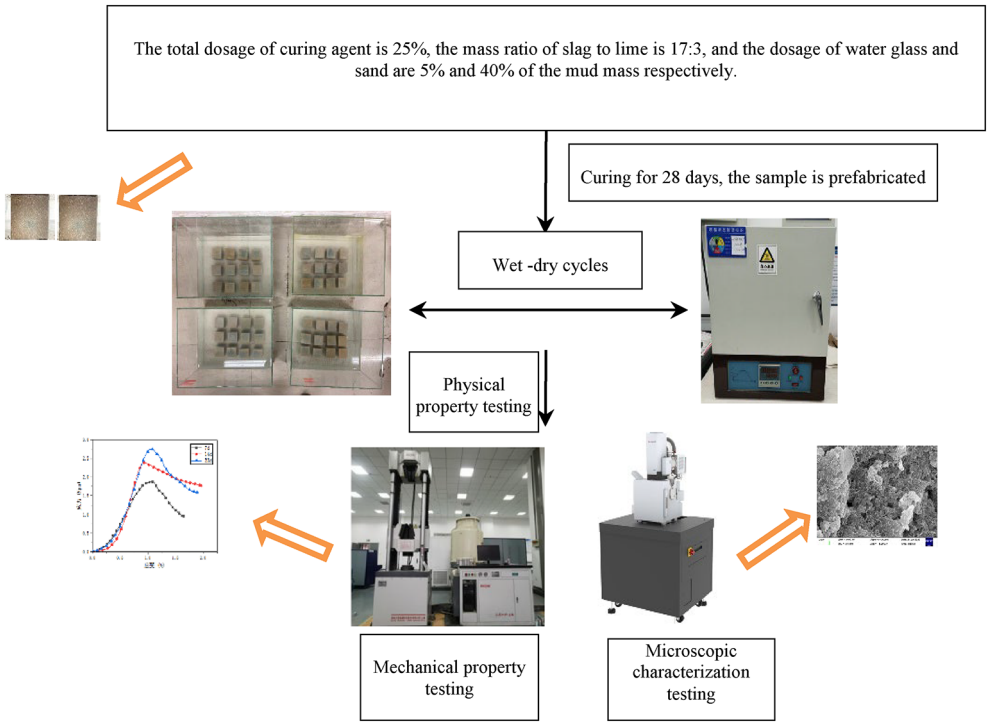

Fig. 5. Test flow chart.

ultrasonic propagation speed in solids is greater than that in the air, which led to the reduction of the average wave velocity of the cured mud.

It can also be seen from Fig. 6 that under the same number of wet and dry cycles, the longitudinal wave velocity of the cured slurry specimen in water is the smallest, while the longitudinal wave velocity in 40 g/L NaCl solution is the largest, and the longitudinal wave velocity of the specimen in water decreases by 9.67%, 15.13%, and 25.80% compared with that in 10 g/L, 20 g/L, and 40 g/L NaCl solutions, respectively, after 10 cycles of wet and dry cycles. This shows that under the same number of wet and dry cycles, the higher the concentration of sodium chloride solution, the greater the longitudinal wave velocity of the cured slurry specimens. The reason is that crystals will be precipitated inside the specimen after soaking in NaCl solution to fill the pores inside the specimen, and the higher the concentration of the solution, the more crystals will be precipitated, resulting in the increase of the longitudinal wave velocity. The reason may be due to the solution immersion, under the influence of the relevant ions in the solution and water, the internal clay material appeared to dissolve in the consolidation, with the increase of the solution concentration this phenomenon is more obvious, further resulting in the change of wave speed.

Rate of change in mass after wet-dry cycling

Under the alternating action of chloride salt and dry and wet cycles, the quality of cured soil samples will change, and the change of its quality can reflect its damage in some way. Therefore, the cured mud specimens after 15 times of wet and dry cycles were selected to study the mass change before and after each cycle, and Fig. 7 reacts the mass change of the specimens under different numbers of wet and dry cycles. In order to reflect the damage of the specimen, the mass change of the specimen before and after the wet and dry cycles was weighed, and the rate of mass change was calculated from Eq. 1.

$$\omega_n = \frac{m_0 - m_n}{m_0} \times 100\% \tag{1}$$

Where ω_n is the mass change rate of the cured mud specimen in %; m_0 is the initial mass of the cured mud specimen before drying and wetting in g; and m_n is the mass of the cured mud specimen after n times of drying and wetting cycles in g.

The relationship between the rate of mass change of the cured mud specimen with the number of wet and dry cycles is shown in Fig. 7.

As can be seen in Fig. 7, the mass of the cured mud specimens all decreased gradually with the increase of the number of wet and dry cycles. As the number of wet and dry cycles increased, the loss of specimen mass also increased, respectively. The reason is that under the action of wet and dry cycles, the soil particles on the surface of the specimen were gradually detached, and the surface holes were increasing, resulting in the reduction of mass and cracks. While soaking in water and sodium chloride solution, water from the cracks into the specimen

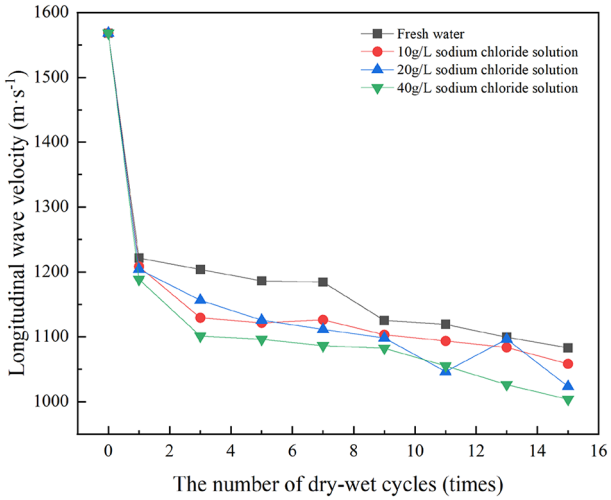

Fig. 6. Longitudinal wave velocity of cured slurry with different number of dry and wet cycles.

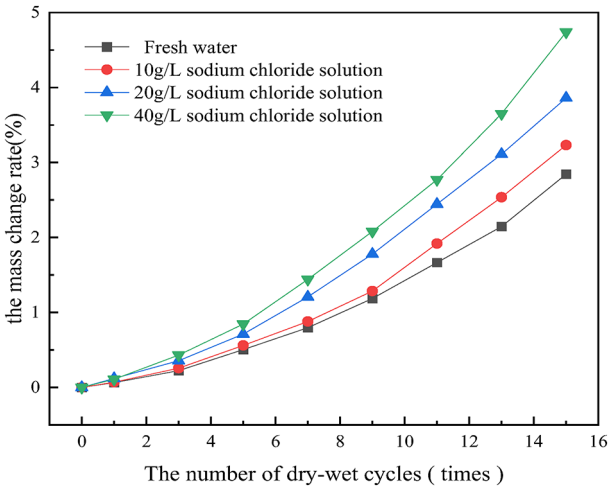

Fig. 7. Mass change of cured slurry specimen as a function of the number of wet-dry cycles.

inside, dissolving the internal bentonite particles and some hydration products, so that it continues to dissolve outflow and the emergence of holes, but also led to the loss of quality.

The relationship between the mass change rate of the cured mud specimen and the number of wet and dry cycles is shown in Fig. 8, from which it can be found that, at the beginning of the wet and dry cycles (0–5 times), the mass change rate of the cured mud specimen under water and different sodium chloride solutions is relatively close, with the increase in the concentration of sodium chloride solution, the rate of change of the mass is also increasing, and after the cycle of 5 times, the mass change rate of the cured mud specimen under water and 10 g/L, 20 g/L, 40 g/L,. After 5 cycles, the mass change rates of cured mud samples under clear water and 10 g/L, 20 g/L, 40 g/L NaCl solution were 0.50%, 0.56%, 0.71%, 0.85%, respectively. In the late stage of wet and dry cycles (7–15 cycles), the difference between the mass change rates of cured mud samples under clear water and different NaCl solutions was increasing, and the mass change rates of cured mud samples under clear water and 10 g/L, 20 g/L, 40 g/L NaCl solution were 2.84%, 2.85% and 2.85%, respectively, after 15 cycles. The mass change rates were 2.84%, 3.23%, 3.86% and 4.74%, respectively. This indicates that with the increase of sodium chloride concentration, the more serious erosion of the solution on the cured mud specimen, so that the specimen in the drying process to produce holes and cracks, and in the sodium chloride solution soaked in the solution from the cracks into the specimen inside, so that the repeated cycle of the specimen surface peeling and hole phenomenon, resulting in the quality of the reduction.

It can also be seen from Fig. 8 that the growth trend of the rate of change in the mass of the cured mud specimens also accelerated with the increase in the number of wet and dry cycles. At the beginning of the wet and dry cycle (0 ~ 5 times), the growth of the rate of change in quality is relatively slow, and the difference in the rate of change in quality of the specimens under different solutions is relatively small; at the later stage of the wet and dry cycle (7 ~ 15 times), the growth of the rate of change in quality accelerates, and the difference in the rate

of change in the quality of the specimens under each solution is also expanding. The reason for this phenomenon is that the overall compactness of the cured mud specimen after 28 days of maintenance age is better, and there are more hydration products such as C-S-H, C-A-H, and C-H in the interior, which bond and wrap the soil particles inside the specimen with each other and fill the holes inside. Therefore, under the action of fewer dry and wet cycles, it is difficult for water to enter the interior of the specimen, and the influence on the specimen is small, the cracks on the surface of the specimen are not obvious, and the appearance of the holes and shedding phenomena are also less, so the growth of the rate of change in quality is small, the growth rate is flat, and the difference in the quality of the specimen under the erosion of different solutions is not large. After a number of wet and dry cycles, due to the entry of water, the internal structure of the sample was damaged, the sample surface cracks appear more, resulting in holes and shedding phenomenon is the main reason for the decline in the quality of the specimen, so at this time, the rate of change in the quality of the growth of the magnitude is larger.

Chloride ion attack depth test

In order to better study the damage mechanism of cured mud under the action of chloride salt and dry-wet cycle from a microscopic point of view, and to explore the chloride ion penetration law, the chloride ion erosion depth test was conducted. After each soaking of the test block, the test block was fully dried, and then the test block was cut from the middle part, scraped off the surface residue, and then sprayed with silver nitrate standard titration solution (concentration of the solution was 0.1 mol/L) to the cutting surface. After placing the test block away from light for a period of time, the $AgNO_3$ reacted with the chlorine ions to produce white AgCl, and the un-reacted $AgNO_3$ would be slightly photolyzed to produce Ag, which was then oxidized to produce black Ag_2O_3, so the cut surface would appear to be black. Ag_2O_3, so the cutting surface will appear white and brown or brown-black two kinds of areas, measure the width of the white area is the depth of chloride erosion. The following figure shows the depth of chloride ion erosion in different concentrations of sodium chloride solutions under different numbers of wet and dry cycles.

From Fig. 9, it can be seen that the depth of chloride ion erosion increases rapidly with the number of wet and dry cycles and then slows down, showing a tendency to stabilize. This indicates that the number of wet and dry cycles of chloride ions (C-H), chloride ions, chloride ions, mainly to the physical adsorption of the main, there have been relevant microscopic studies have shown that: hydration products of the internal structure of the dense, gel pore occupies a large proportion of larger than a large specific surface area and a strong surface energy, increasing the adsorption capacity of the chloride ion, while the pore solution of the pore, the depth of chloride ion erosion. The concentration of chloride ions in the pore solution plays a decisive role in the adsorption process. The alternation of wet and dry accelerated the transport of chloride ions, with the increase of the number of wet and dry cycles, the surface pore dryness of the test block increased, the pore liquid concentration increased to saturation, so that the surface capillary pressure increased, in the wetting process, due to the existence of a gradient of pore liquid saturation inside the test block, the resulting capillary pressure made the chloride ion invasion rate increased, the increase in the content of free chloride ions inside the test block increased the chlorine ions adsorbed. Adsorption. However, with the continuous increase of the number of wet and dry cycles, the adsorption capacity of the gelatinized material of the specimen on the surface of the specimen for chloride ions decreases under the same soaking time, so that the content of free chloride ions inside the specimen decreases, and the growth of the erosion depth slows down. The greater the depth of penetration of chloride ions, the more serious the weakening of the cementing ability of the internal cementitious material, which explains why the rate of reduction of the strength and quality of cured mud slows down with the increase in the number of wet and dry cycles, and the actual performance of the text and better.

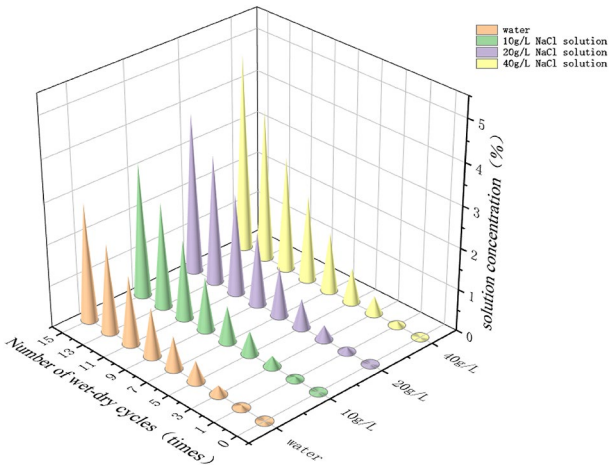

Fig. 8. Rate of change in mass of cured slurry specimens as a function of the number of wet - dry cycles.

Apparent morphology after wet-dry cycling

The specimens that reached the number of wet and dry cycles were removed, and the changes in the apparent morphology of the specimens were observed to understand the surface damage of the cured mud after chloride salt erosion and wet and dry cycles. As shown in Table 2.

Analysis of uniaxial mechanical parameters and deformation parameters after dry-wet cycles

Figure 10 shows the results of the unconfined compressive strength tests of the cured mud specimens at each number of cycles and at different NaCl concentration solutions, where 0 wet and dry cycles are the results of the control group.

As can be seen in Fig. 10, the unconfined compressive strength of cured mud in both clear water and sodium chloride in two different erosive environments decreased continuously with the increase of the number of wet and dry cycles. After 15 wet and dry cycles, the unconfined compressive strength of cured mud in water and 10 g/L, 20 g/L, 40 g/L NaCl solution decreased from 4.33 MPa in the control group to 3.05 MPa, 2.75 MPa, 2.56 MPa, 2.04 MPa, respectively. The main reason for the decrease in strength is that, with the increase in the number of wet and dry cycles, the surface cracks appeared on the surface of the cured mud sample and the accompanying cracks appeared on the surface of the mud sample. Cracks appeared on the surface, accompanied

	Experimental condition	Analysis of changes in apparent morphology
Number of dry-wet cycles	 (a) 1 time  (b) 3 times  (c) 5 times  (d) 7 times  (e) 9 times  (f) 11 times  (g) 13 times  (h) 15 times	After wet and dry cycles, holes and cracks gradually appeared on the surface of the cured mud specimens in clear water. The surface of the specimen after 1 cycle is relatively smooth and complete, with no obvious holes and cracks; the surface of the specimen after 7 cycles has developed obvious holes and cracks; the specimen after 15 cycles has the largest number of holes and cracks, and the corners have already developed obvious detachment, with the most serious surface breakage. It can be seen that the more the number of dry-wet cycles, the more serious the breakage of the surface of the cured mud specimen. This is due to the continuous and repeated immersion and evaporation of water during the dry-wet cycles, which gradually dissolves the hydration product $Ca(OH)_2$ in the original specimen and causes the continuous precipitation of Ca^{2+} in the curing slurry, leading to the appearance of holes in the specimen. At the same time, the specimen immersed in water due to continue to occur part of the hydration reaction, the consumption of water and produce hydration products, so that the specimen internal expansion stress, and in the drying process, due to the evaporation of water, the specimen volume and began to reduce, and so on and so forth, to produce the phenomenon of breakage.
Different chloride concentrations after 15 dry-wet cycles	 (a) clear water  (b) 10g/L solution of sodium chloride  (c) 20g/L solution of sodium chloride  (d) 40g/L solution of sodium chloride	After 15 dry-wet cycles, the surfaces of the specimens in both water and three concentrations of sodium chloride solutions showed varying degrees of holes, cracks, and breakage. The holes and cracks on the surface of the specimens in the water were fewer and less damaged than those in the NaCl solution; the surface of the specimens in the 40 g/L NaCl solution was the most seriously damaged, with the most holes and cracks, and the corners had been more seriously detached. It was able to find that as the concentration of NaCl increased, the more severe the surface breakage of the cured slurry under the action of dry-wet cycling. The reason is that Cl^- in sodium chloride solution has strong permeability [28], which can weaken the cementing ability of the hydration products inside the cured mud, while Na^+ in the solution can weaken the bond between the soil of the cured mud [29], which makes the structure loose and cracks appear. Therefore, the higher the concentration of sodium chloride solution, the more severe the surface breakage of the cured mud.

Table 2. Apparent morphology under different dry-wet cycles and apparent morphology in different solutions.

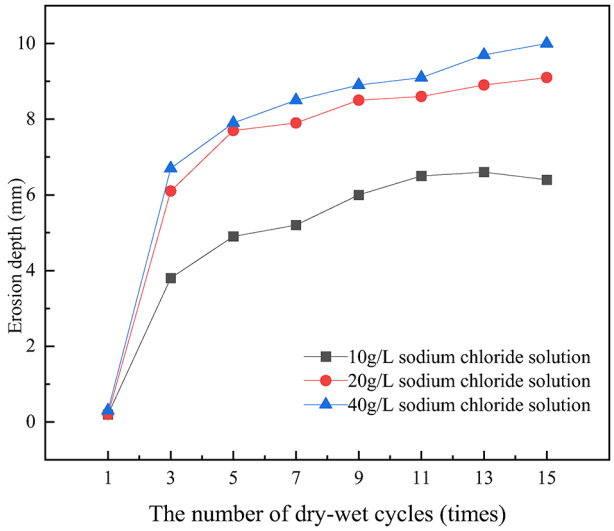

Fig. 9. Depth of chloride ion erosion in sodium chloride solutions with different concentrations under different numbers of wet and dry cycles

by the shedding of the surface soil particles, due to the continuous expansion of the cracks to the interior, which had a relatively large impact on the strength of the specimen, at the same time, the specimen in the process of soaking absorbed water and the process of water migration[30], the absorbed water filled the pores or capillaries inside the cured mud, and in the process of drying, these waters were evaporated, so that the repeated dry and wet cycle led to the destruction of the internal structure of the specimen, the gradual development and expansion of pores and cracks, and ultimately the gradual reduction of the strength of the specimen.

Further from Fig. 10, it can be seen that under the same number of wet and dry cycles, the strength of the cured mud specimen in clear water is the highest, and the higher the concentration of sodium chloride solution, the lower the unconfined compressive strength, after 15 times of wet and dry cycles, the longitudinal wave velocity of the specimen in 40 g/L sodium chloride solution decreased by 33.11%, 25.82%, compared with that of the clear water and 10 g/L, 20 g/L sodium chloride solution, respectively, 20.31%. It shows that the unconfined compressive strength of the cured mud changes after erosion by sodium chloride solution, and the change is greater with the higher concentration. The main reason for this phenomenon is that when the specimen is immersed in sodium chloride solution, due to osmotic pressure, the chloride salt solution will gradually penetrate into the interior of the specimen and continuously generate new crystals, and the higher the concentration of chloride salt, the faster the penetration rate, after many wet and dry cycles, the chloride salt solution penetrated into the interior of the specimen due to the generation of more crystals will generate crystallization pressure[31], so that the specimen suffers from expansion and damage and continuously generate enlarged cracks. The higher the concentration of sodium chloride, the greater the damage to the specimen, so the lower the strength.

According to the results in Fig. 9, it can be seen that the relationship between the change in unconfined compressive strength with the number of wet and dry cycles is approximately linear, whether the cured mud specimens in clear water or chloride salt solution, so Eq. 2 was used to fit the analysis in order to better predict the change in compressive strength with the number of wet and dry cycles.

$$\sigma_u = a + bt \tag{2}$$

Where σ_u is the unconfined compressive strength of the cured mud specimen in MPa; a and b are the parameters obtained from the fitting; and t is the number of wet and dry cycles in times.

The fitting results are shown in Fig. 11; Table 3.

It can be seen from Fig. 11; Table 3 that the fitting results basically conform to the change rule of the cured mud unconfined compressive strength, and the R2 in both clear water and different chloride salt solutions reaches more than 0.96, which is a good fitting result. Using the fitting method, the values of the cured unconfined compressive strength under different dry and wet cycle conditions were obtained to reveal its durability under the combined effect of chloride salt erosion and dry and wet cycle.

The deformation modulus can be calculated to show the ability of the cured mud to resist elastic deformation after the test, so the deformation modulus E_{50} was used to characterize the deformation properties of the cured mud, and Fig. 12 reflects the variation of the deformation modulus of the cured mud with the number of dry and wet cycles under different erosive conditions, in which the 0th cycle is the deformation modulus of the control group specimen.

As can be seen from Fig. 12, the deformation modulus of the cured mud specimens in clear water and different solutions showed a gradual decrease with the increase of the number of wet and dry cycles. After 9 times of wet and dry cycles, the deformation modulus of cured mud in water and 10 g/L, 20 g/L, 40 g/L NaCl solution decreased by 32.55%, 37.94%, 38.57%, and 42.78%, respectively, compared with that of the control

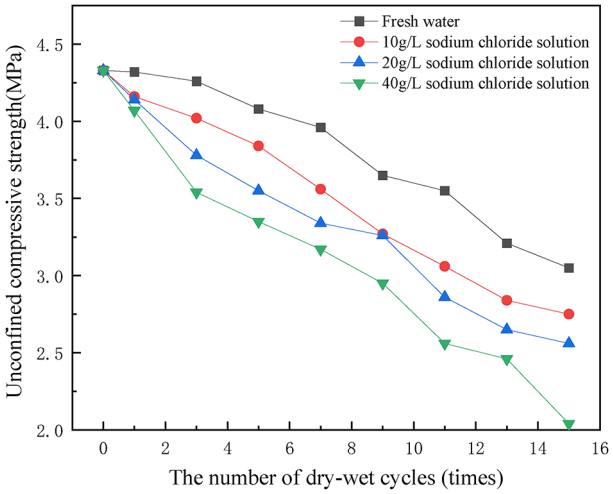

Fig. 10. Variation of unconfined compressive strength of cured mud with different number of dry and wet cycles.

Different erosive solutions	Fitted formula	R^2
clear water	$\sigma_u = -0.089 + 4.459$	0.966
10 g/L solution of sodium chloride	$\sigma_u = -0.110 + 4.319$	0.991
20 g/L solution of sodium chloride	$\sigma_u = -0.117 + 4.221$	0.982
40 g/L solution of sodium chloride	$\sigma_u = -0.140 + 4.160$	0.977

Table 3. Fitting results of unconfined compressive strength of solidified mud under different dry wet cycles.

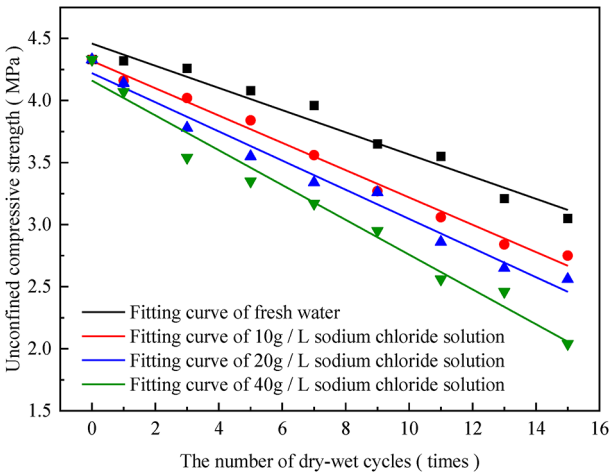

Fig. 11. Fitted curve of unconfined compressive strength of cured mud with different number of wet and dry cycles.

group, and the decrease of deformation modulus of specimens in 9–15 times of wet and dry cycles gradually leveled off. After 15 wet and dry cycles, the deformation modulus of the cured slurry in water and 10 g/L, 20 g/L, and 40 g/L NaCl solution decreased by 11.65%, 10.89%, 14.01%, and 13.73%, respectively, compared with that after 9 wet and dry cycles. The reason for the gradual decrease in the deformation modulus is that the internal structure of the specimens changed after the wet and dry cycles, producing pores and cracks, which led to the decrease in strength and deformation modulus.

It can also be seen from Fig. 12that, under the same number of wet and dry cycles, the decrease of deformation modulus of cured mud specimens in water was smaller than that in NaCl solution, and the decrease of deformation modulus of specimens in 40 g/L NaCl solution was the largest, and the decrease of deformation modulus of specimens in 40 g/L NaCl solution was 17.6% compared with that of specimens in water and 10 g/L

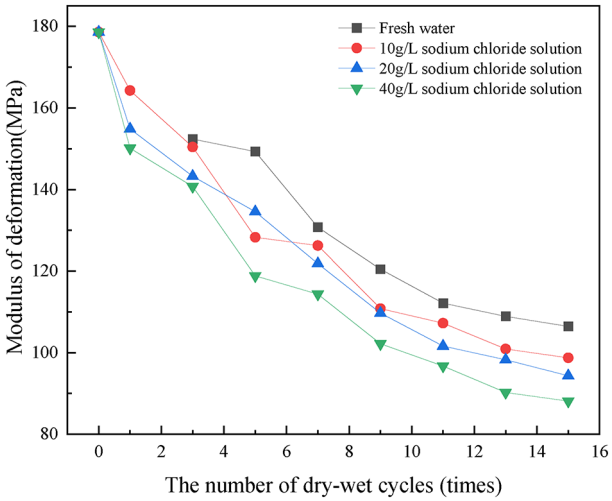

Fig. 12. Deformation modulus of cured slurry with different number of wet and dry cycles.

and 20 g/L NaCl solution, respectively, after 15 times of wet and dry cycle tests. The modulus of deformation of the specimens in 40 g/L NaCl solution decreased by 17.18%, 10.73%, and 6.56%, respectively. It can be seen that as the concentration of NaCl increases, the decrease in the modulus of deformation of the specimens is greater. This is because the surface water loss rate of cured mud during drying is higher than the internal water loss rate during wet and dry cycles, due to the difference between the internal and external water content, resulting in greater shrinkage deformation of the surface than the internal, which causes cracks in the specimen, and after soaking in sodium chloride solution, the solution will enter the specimen along the cracks and erode the internal structure, causing irrecoverable deformation of the specimen and resulting in breakage[32], after many cycles, resulting in the broken deformation of the specimen in sodium chloride solution is more serious, and the higher the concentration of the solution, the more serious the degree of erosion, the greater the magnitude of the decrease in deformation modulus.

Microstructure of specimens after dry - wet cycles

Figure 13 shows the microstructure of the cured mud specimens after 15 cycles of wet and dry cycles in control and fresh water and different solutions.

From Fig. 13(a), it can be seen that there are only few holes and cracks inside the untested control specimen with more hydration products. Hydration products such as flocculent hydrated calcium silicate gel (C-S-H), plate-like calcium hydroxide crystals (C-H), and needle-and-rod calcium alumina crystals (AFt) can be found[33,34], and these hydration products make the internal structure of the cured mud denser by bonding with each other and filling up the internal pore space, so that the microscopic manifestation is less pores and cracks. Figure 13(b) shows the microstructure of the specimen under water immersion. After 15 cycles of wet and dry cycles under water immersion, it can be found that more pores and cracks appeared in the specimen, compared with the control specimen, the number of pits and grooves increased, and the hydration products decreased, and the adhesion between soil particles weakened, and the internal structure tended to be loosened. This is because under repeated dry and wet cycles, the water in the specimen will enter the specimen interior through the crevices, which dissolves part of the material and hydrolyzes part of the cementitious material, making the internal pores and cracks expanding, leading to the appearance of more pores and cracks.

Figure 13 (c), (d), and (e) shows the microstructure of the cured mud specimens after 15 dry and wet cycles in 10 g/L, 20 g/L, and 40 g/L NaCl solution, respectively, and it can be found that more pores and cracks appeared inside the specimens in the chlorinated salt solution, and with the increase of NaCl concentration, the hydration products decreased, and the more pores and cracks appeared, and in the 40 g/L NaCl solution, larger pores and cracks have appeared inside the specimen, compared with the specimens in 10 g/L and 20 g/L NaCl solution, the structure is more loose, the hydration products are less, and the bonding ability is greatly weakened. The reason is that the higher the concentration of NaCl, the more serious erosion of cured mud specimens, and inhibit the generation of internal hydration products, reducing the bonding capacity between soil particles and hydration products, resulting in the increase of cracks and pores.

Conclusion

In this paper, the unconfined compressive strength, change in apparent morphology, and rate of mass change of cured mud specimens after testing were investigated by dry and wet cycling tests of cured mud under erosion with different concentrations of sodium chloride solutions. It was also analyzed microscopically in conjunction with scanning electron microscope tests to understand its durability under chloride salt erosion and wet/dry cycling coupling. The following main conclusions were obtained:

(1)With the increase of the number of wet and dry cycles, holes and cracks gradually appeared on the surface of the cured mud specimens in clear water, and the more the number of wet and dry cycles, the more serious

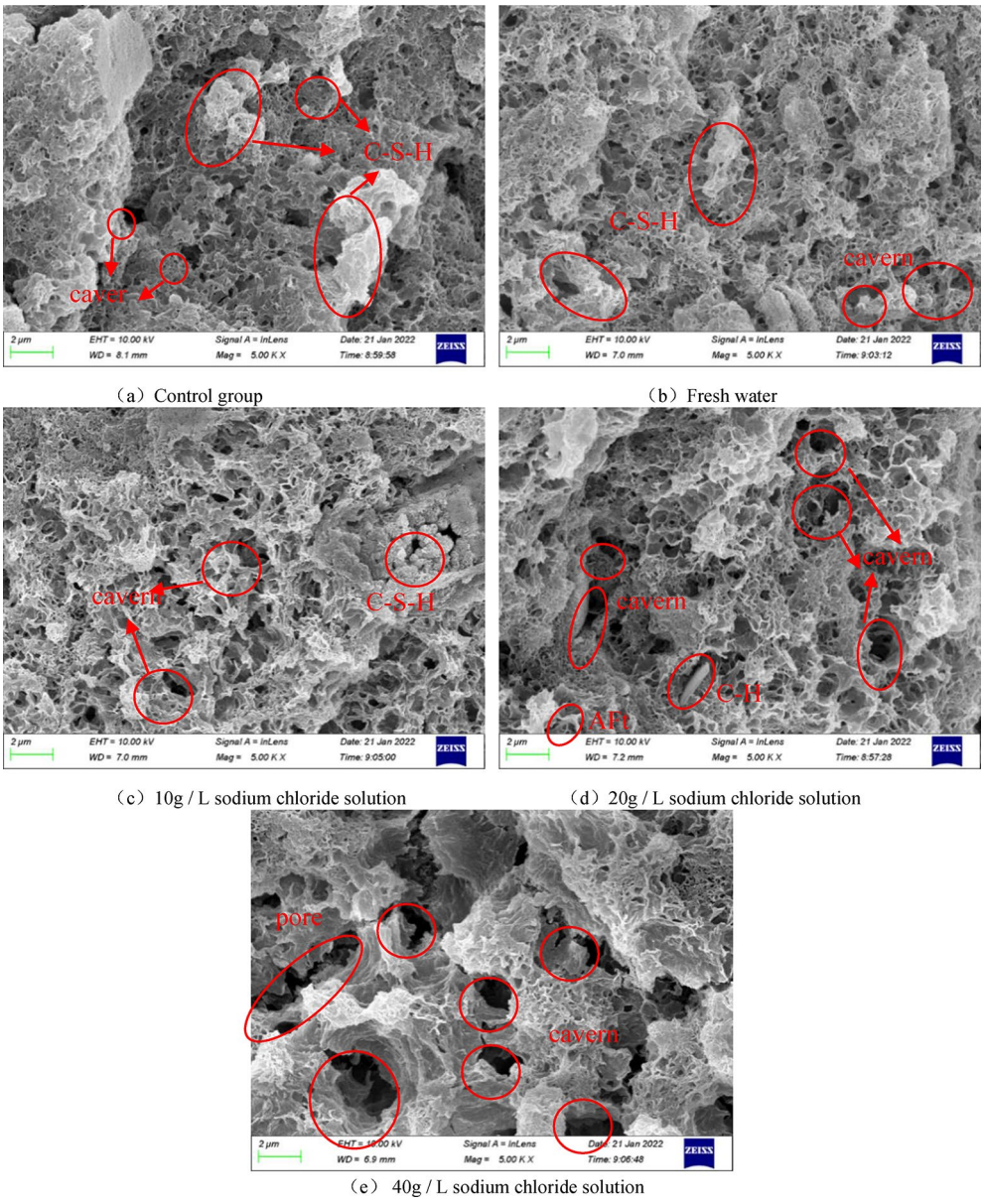

Fig. 13. Microstructure diagram of solidified mud after 10 dry and wet cycles

the degree of damage on the surface of the specimens; after 15 wet and dry cycles, the surface of cured mud specimens under different sodium chloride concentration solutions showed different degrees of cracks, holes, and damage, and the higher the concentration of sodium chloride solution, the more serious the degree of damage on the surface of the specimens. The higher the concentration of NaCl solution, the more serious the damage on the surface of the specimen.

(2) With the increase of the number of wet and dry cycles, the mass of the cured mud samples in water and different concentrations of sodium chloride solution gradually decreased, and the growth of the rate of change of mass accelerated with the increase of the number of wet and dry cycles. Under the same number of wet and dry cycles, when the concentration of sodium chloride increases, the erosion phenomenon of the solution on the specimen is more obvious, and the mass loss of the specimen will also increase.

(3) The unconfined compressive strength of the cured mud specimens under the erosion of water and different concentrations of sodium chloride solution decreased with the increase of the number of wet and dry cycles; under the same number of wet and dry cycles, the higher the concentration of sodium chloride solution, the lower the unconfined compressive strength of the specimens. And the strength changes of cured mud under different cycle times were derived by fitting equations.

(4) Through the scanning electron microscope microscopic test, it was analyzed that the internal structure of the control specimen was dense, with only few pores and cracks, more hydration products, and the presence of a large number of hydration products such as hydrated calcium silicate gel (C-S-H), calcium hydroxide crystals (C-H), and calcite alumina crystals (AFt); the specimen under the water immersion appeared to have a larger

number of pores and cracks in the interior, with a reduction of hydration products, and the structure tended to be loosened. The cured mud specimen under chloride salt erosion and wet/dry cycle coupling has fewer hydration products, more cracks and pores, weakened bonding ability between soil particles, looser structure, and poorer integrity, and the higher the concentration of NaCl, the more serious the microscopic damage inside the specimen.

Data availability

Data can be obtained from the Corresponding author.

Received: 4 October 2024; Accepted: 9 December 2024
Published online: 07 January 2025

References

1. Fernando, P. T . et al. Investigations about the effect of aggregates on strength and microstructure of geopolymeric mine waste mud binders. *Cem. Concr. Res.* **37**(6), 933–941 (2007).
2. Gao, S. H. et al. Experimental and field study on treatment waste mud by in-situ solidification. Proceedings of the Institution of Civil Engineers - Municipal Engineer, 173(4), 1–23 (2018).
3. Rykusova, N. et al. Identification of properties of recycled highdensity polyethylene composites when filled with waste mud solids. *Eastern-European J. Enterp. Technol.* **2**(10(98)), 55–60 (2019).
4. Wu, D. Q. et al. Research progress of solid waste recycling for land reclamation technology in Singapore. *Environ. Sci. Res*. **31**(07), 1174–1181 (2018).
5. Guang, L. et al. Immobilization of heavy metal contaminated soil by different cementation materials. *Res. J. Environ. Sci.* **23**(1), 106–111 (2010).
6. Zentar, R. et al. Utilization of siliceous-aluminous fly ash and cement for solidification of marine sediments. *Constr. Build. Mater.* **35**, 856–863 (2012).
7. Yi, Y. et al. Test on alkali-activated ground granulated blast-furnace slag (GGBS) for Lianyungang soft soil stabilization. *Chin. J. Rock Mechan. Eng.* **32**(9), 1820–1826 (2013).
8. Ou, X. D. et al. Biological consolidation test study of hydraulic fill for land reclamation at North Bay of Guangxi Province. *Rock Soil Mech.*. **36**(1), 28–33 (2015).
9. Zhu, W. et al. Soil-water transfer mechanism for solidified dredged materials. *J. Geotech. GeoEnviron. Eng.* **133**(5), 588–598 (2007).
10. Huang, Y. et al. Change of mechanical behavior between solidified and remolded solidified dredged materials. *Eng. Geol.* **119**(3), 112–119 (2011).
11. Zhang, T. J. et al. Change law of water content of dredged clays treated by quick lime. *Rock. Soil. Mech.* **30**(9), 2775–2779 (2009).
12. Chan, C. M., et al . A fundamental parametric study on the solidification of Malaysian dredged marine soils. *World Appl. Sci.* **24**(6), 784–793 (2013).
13. Chen, W. J. et al. Optimization of microstructure and mechanical performance of clay-rich sand-washing slurry-based geopolymers. *Appl. Clay Sci.* **260**, 107551–107551 (2024).
14. Zhang, J. J. et al. Study of evolution law off issures of expansive clay under wetting and drying cycles. *Rock Soil Mech.* **32**(9), 2729–27340 (2011).
15. Zhang, W. et al. Experimental study on shear strength characteristics of sulfate saline soil in Ningxia region under long-term freeze-thaw cycles. *Cold Reg. Sci. Technol.* **160**, 48–57 (2019).
16. Lv, Q. et al. A study on the effect of the salt content on the solidification of sulfate saline soil solidified with an alkali-activated geopolymer. *Constr. Building Mater.* **176**(10), 68–74 (2018).
17. He, J. et al. Mechanical properties of alkali slag-slag solidified sludge in eroded environment. *Hydrogeol. Eng. Geol.* **46**(06), 83–89 (2019).
18. Maio, D. Exposure of bentonite to salt solution: osmotic and mechanical effects. *Geotechnique* **46**(4), 695–707 (1996).
19. Di, M. et al. Shear displacements induced by decrease in pore solution concentration on a pre-existing slip surface. *Eng. Geol.* **200**, 1–9 (2016).
20. Peng, T. Study on the strength degradation law and service life of grouting materials for subsea tunnels. *Hydrogeological Eng. Geol.* **38**(01), 65–68 (2011).
21. Bian X. et al. Effect of drying-wet cycle on physical and mechanical properties of polymer absorbent resin solidified mud soil. *China J. High. Transp*. **36**(10), 55–63 (2023).
22. Zhang, J. S. et al. Experimental study on the characteristics of slag-lime-water glass composite cured mud. *Arab. J. Geosci.* **15**(18), 1–9 (2022).
23. Ou, M. X. et al. Experimental study on expansive soil preparation engineering mud. *J. Northwest. F Univ. (Natural Sci. Edition)*. **04**, 44 (2016).
24. Cong, A. S. et al. Design, Construction and Application of deep Foundation pit anti-seepage body [M]. Beijing: Intellectual Property (2012).
25. Yang, H. R. et al. Study on the damage mechanism of microstructure of sand conglomerate in Maijishan Grottoes by freeze-thaw cycles. *Chin. J. Mech. Eng.* **40**(03), 545–555 (2021).
26. Wu, Q. Y. et al. Frost resistance and damage model of BSFC under Freeze-Thaw Cycles. *J. Building Mater.* **24**(06), 1169–1178 (2021).
27. Huang, X. Study on physical and mechanical properties and damage model of sandstone under acid dry wet cycle. *Anhui University of Science & Technology* (2020).
28. Malliou, O. et al. Properties of stabilized/solidified admixtures of cement and sewage sludge[J]. *Cement Concr. Compos.* **29**(1), 55–61 (2007).
29. Cha, F. S. et al. Experimental Study on Strength and Microscopic Characteristics of Cement Solidified lead Contaminated soil under NaCl erosion Environment. *Rock Mech. Rock Eng.* **34**(S2), 4325–4332 (2015).
30. Zhang, L. J. Comparative Experimental Study on Expansibility and Shrinkage of Expansive soil. *Southwest Jiaotong University* (2014).
31. Su, X. P. et al. Experimental study on durability of concrete under single salt erosion and freeze-thaw cycles. *Industrial Building.* **44**(09), 110–113 (2014).
32. Hu, C. M. et al. Experimental study on strength deterioration model of compacted loess under wetting-drying cycles. *J. Rock. Mech. Eng.* **37**(12), 2804–2818 (2018).
33. Gu X. J.et al. Improvement of mechanical properties and condensation mechanism of calcium hydroxide on slag alkali-activated materials. *J. Jiangsu Vocat. Tech. Coll. Archit.* **24**(03), 31–38 (2024)
34. Zhang, M. et al. Basic mechanical properties and microscopic properties of alkali-activated slag/fly ash desert sand concrete. *Materials Reports* 1–26(2024)

Acknowledgements
The work described in this article was supported by the Anhui Provincial Higher Education Science Research Project (2023AH051219).

Author contributions
Songtao Zhang : Writing – review & editing, Writing – original draft, Methodology. Jianyong Pang: Writing – review & editing, Methodology, Funding acquisition, Data curation, Conceptualization. Jinsong Zhang: Writing – review & editing, Writing – original draft, Visualization, Software, Methodology, Formal analysis, Data curation, Conceptualization. Changwei Zhou: Writing – review & editing, Writing – original draft, Visualization, . Yaxing Wang: Methodology, Formal analysis, Data curation.

Declarations

Competing interests
The authors declare no competing interests.

Additional information
Correspondence and requests for materials should be addressed to P.J.

Reprints and permissions information is available at www.nature.com/reprints.

Publisher's note Springer Nature remains neutral with regard to jurisdictional claims in published maps and institutional affiliations.